Mineralogical Magazine, October 2013, Vol. 77(7), pp. 2901–2912

The crystal structure of chalcoalumite: mechanisms of Jahn-Teller-driven distortion in $^{[6]}Cu^{2+}$-containing oxysalts

F. C. HAWTHORNE* AND M. A. COOPER

Department of Geological Sciences, University of Manitoba, Winnipeg, Manitoba R3T 2N2, Canada

[*Received 22 June 2013; Accepted 23 July 2013; Associate Editor: S. Mills*]

ABSTRACT

The crystal structure of chalcoalumite, ideally $Cu^{2+}Al_4(SO_4)(OH)_{12}(H_2O)_3$, monoclinic, $P2_1/n$, $Z = 4$: a 10.228(3), b 8.929(3), c 17.098(6) Å, β 95.800(11)°, V 1553.6(1.5) Å^3, has been refined to R_1 = 3.08% for 4,022 unique observed (4σ) reflections collected on a Bruker D8 three-circle diffractometer equipped with a rotating-anode generator, multilayer optics and an APEX-II CCD detector. In the structure of chalcoalumite, there is one *S* site, tetrahedrally coordinated by four O anions, with <*S*–O> = 1.472 Å. There are four *Al* sites with site-scattering values in accord with occupancy by Al and <*Al*–O> distances of 1.898–1.919 Å. There is one *Cu* site occupied by Cu^{2+} and coordinated by six anions in the [4 + 2] arrangement typical for octahedrally coordinated Cu^{2+}. The short <*Cu*–O> distance of 2.086 Å is in accord with the low degree of bond-length distortion of the Cu octahedron. There are 19 anion sites: 4 sites are occupied by O atoms that are bonded to the S cation, 12 sites are occupied by (OH) groups that bond to all octahedrally coordinated cations, and 3 sites are occupied by (H_2O) groups that are held in the structure solely by hydrogen bonding. The structure of chalcoalumite consists of interrupted sheets of edge-sharing Al and Cu octahedra of the form $[Cu^{2+}Al_4(OH)_{12}]^{2+}$ that intercalate layers of (SO_4) tetrahedra and (H_2O) groups. Chalcoalumite is a member of the nickelalumite group.

$Cu^{2+}\varphi_6$ ($\varphi = O^{2-}, (OH)^-, (H_2O)^0$) octahedra show a wide range of bond-length distortion away from the holosymmetric arrangement, driven by spontaneous symmetry-breaking of the degenerate electronic ground-state in holosymmetric octahedral coordination. Here, we examine the structural mechanisms that allow large octahedron distortions of this type. There are two mechanisms: (1) coupling of (usually parallel) octahedron distortions to a vibrational phonon, inducing a (often ferroelastic) phase transition in M^{2+}-Cu^{2+} solid-solutions; (2) cooperative orientational disorder, where bond topology (polyhedron linkage) allows large differences in bond lengths within polyhedra to accord with the valence-sum rule of bond-valence theory.

KEYWORDS: chalcoalumite, crystal structure, sulfate, nickelalumite group.

Introduction

CHALCOALUMITE, ideally $Cu^{2+}Al_4(SO_4)(OH)_{12}(H_2O)_3$, is a sulfate mineral first described by Larsen and Vassar (1925) from Bisbee, Arizona, USA, where it occurs as matted fibres that form crusts on stalagtites of limonite. Larsen and Vassar note that twinning is common, and this was confirmed by Williams and Khin (1971) on chalcoalumite from the Sacramento pit at Bisbee. The latter material differs significantly from the fibrous chalcoalumite described by Larsen and Vassar (1925), consisting of "small, highly perfect crystals (0.5 mm in diameter)" that occur in vugs in dense quartz-goethite gossan or in pockets of coarse fibrous malachite (Williams and Khin, 1971). Chalcoalumite is a member of the nickelalumite group (Table 1), the structural

* E-mail: frank_hawthorne@umanitoba.ca
DOI: 10.1180/minmag.2013.077.7.02

© 2013 The Mineralogical Society

TABLE 1. The minerals of the nickelalumite group.

Mineral name	Formula	Space group	*a* (Δ)	*b* (Δ)	*c* (Δ)	β (E)	*Z*	Ref.
Nickelalumite*	$NiAl_4(OH)_{12}(SO_4)(H_2O)_3$	$P2_1/n$	10.2567(5)	8.8815(4)	17.0989(8)	95.548(1)	4	(1)
Kyrgyzstanite	$ZnAl_4(OH)_{12}(SO_4)(H_2O)_3$	$P2_1/n$	10.246	8.873	17.220	96.41	4	(2)
Mbobomkulite	$(Ni,Cu^{2+})Al_4(OH)_{12}[(NO_3),(SO_4)]_2(H_2O)_3$	–	10.171	8.865	17.145	95.37	4	(3)
Hydrombobomkulite	$(Ni,Cu^{2+})Al_4(OH)_{12}[(NO_3)_2,(SO_4)](H_2O)_{12}$	–	10.145	17.155	20.870	90.55	4	(3)
Chalcoalumite	$CuAl_4(OH)_{12}(SO_4)(H_2O)_3$	$P2_1/n$	10.228(3)	8.929(3)	17.098(6)	95.80(1)	4	(4)
Alvanite	$(Zn,Ni)Al_4(OH)_{12}(VO_3)_2(H_2O)_2$	$P2_1/n$	17.808(8)	5.132(3)	8.881(4)	92.11(3)	2	(5)
Ankinovichite	$(Ni,Zn)Al_4(OH)_{12}(VO_3)_2(H_2O)_2$	$P2_1/n$	17.8098(8)	5.1228(2)	8.8665(4)	92.141(1)	2	(6)

* Bolded mineral names: the structures have been refined.

References: (1) Uvarova *et al*. (2005), Karpenko *et al*. (2004*b*); (2) Agakhanov *et al*. (2005); (3) Martini (1980); (4) This work; Williams and Khin (1971), Larsen and Vassar (1925); (5) Pertlik and Dunn (1990); (6) Karpenko *et al*. (2004*a*).

aspects of which have been examined by Uvarova *et al.* (2005), and the infrared spectrum for which was reported by Frost *et al.* (2010). For many years prior to solution of the nickelalumite structure, we tried to characterize the structure of chalcoalumite but were unsuccessful due to the size of the available crystals. This situation changed with our acquisition of a rotating-anode instrument, and the resulting structure is presented here.

X-ray data collection

X-ray-diffraction data were collected with Mo*K*α X-radiation on a Bruker D8 three-circle diffractometer equipped with a rotating-anode generator, multilayer optics and an APEX-II CCD detector using a crystal of chalcoalumite from Bisbee. The intensities of 60,757 reflections (18,173 in the Ewald sphere) were collected to 60º 2θ using 20 s per 0.2º frame with a crystal-to-detector distance of 5 cm. An empirical absorption correction (SADABS, Sheldrick, 2008) was applied, and the data were corrected for Lorentz, polarization and background effects. The refined unit-cell parameters (Table 2) were obtained from 4,018 reflections with $I > 10\sigma I$.

Structure solution and refinement

Preliminary examination of the *E* statistics gave $|E^2 - 1| = 1.295$, indicating a centrosymmetric structure not consistent with the space group $P2_1$ assigned by Williams and Khin (1971). Systematic absences uniquely indicated the space group $P2_1/n$, and refinement proceeded on this basis with the *SHELXTL* version 5.1 system of programs (Bruker, 1997). The O(18) site showed large displacement parameters and the associated H atoms could not be detected in the difference-Fourier map. The O(18) anion was split into three partly occupied sites, O(18), O(18A) and O(18B), the positional coordinates of which were refined in the final cycles of refinement. There were no significant reductions in the *R* indices associated with this splitting. At the later stages of refinement, difference-Fourier maps showed single weak-density maxima ~1 Å from the O(1)−O(12) anions that incident bond-valence sums indicate are (OH) groups, and pairs of weak-density maxima ~1 Å from the O(17) and O(19) anions that incident bond-valence sums indicate are (H_2O) groups. These maxima are in accord with the H positions given by Uvarova *et al.* (2005): they were entered into the structure

TABLE 2. Miscellaneous refinement data for chalcoalumite.

a (Å)	10.228(3)	Crystal size (μm)	10 × 60 × 80
b	8.929(3)	Radiation	Mo*K*α
c	17.098(6)	No. of intensities	60757
β (°)	95.800(11)	No. of reflections in Ewald sphere	18173
V (Å^3)	1553.6(1.5)	No. unique reflections	4567
Space group	$P2_1/n$	No. with ($F_o > 4\sigma F$)	4022
Z	4	R_{merge} (%)	1.9
	R_1 (%)	3.08	
	wR_2 (%)	10.07	
Cell content: $Cu^{2+}Al_4(OH)_{12}(SO_4)(H_2O)_3$			

$R_1 = \Sigma(|F_o| - |F_c|)/\Sigma|F_o|$

w$R_2 = [\Sigma w(F_o^2 - F_c^2)^2/\Sigma w(F_o^2)^2]^{½}$, $w = 1/[\sigma^2(F_o^2) + (0.0538\ P)^2 + 1.12\ P]$ where $P = (\max(F_o^2,0) + 2F_c^2)/3$.

model as H atoms and their parameters were refined with the soft constraint that the O–H distance be ~0.98 Å. The final model refined to R_1 and wR_2 indices of 3.08% (4,022 observed reflections, 311 variable parameters) and 10.07% (4,567 reflections, 311 variable parameters), respectively. The maximum and minimum residual densities in the final difference-Fourier maps are +0.82 and −0.89 eÅ^{-3}. Details of the data collection and structure refinement are given in Table 2, final atom parameters are given in Table 3, selected interatomic distances and angles in Table 4, and bond valences in Table 5. A table of structure factors has been deposited with the Principal Editor of *Mineralogical Magazine* and are available from www.minersoc.org/pages/e_journals/dep_mat_mm.html.

Chemical composition

A crystal of chalcoalumite was mounted in epoxy, polished, and examined using a Cameca SX-100 electron microprobe operating in both energy-dispersive (EDS) and wavelength-dispersive (WDS) modes with an accelerating voltage of 15 kV, a specimen current of 10 nA, and a beam size of 20 μm. Preliminary EDS examination showed signals for Cu, Al and S only. Subsequent WDS analysis for Zn, Fe, Mg and Mn with count times on peak and background of 30 s showed that all these elements are below detection limit.

Description of the structure

Cation sites

There is one *S* site with a site-scattering value compatible with occupancy by S^{6+} and tetrahedrally coordinated by O anions with a <S–O> distance of 1.472 Å, close to the grand <S–O> distance of 1.473 Å found for sulfate minerals by Hawthorne *et al.* (2000). There are four *Al* sites with site-scattering values and mean bond lengths (1.898 to 1.918 Å) characteristic of occupancy by Al. There is one *Cu* site with a site-scattering value and mean bond length compatible with occupancy by Cu^{2+}.

Anion sites

Inspection of the bond-valence table of chalcoalumite (Table 5) shows that the four anions coordinating the *S* site have incident bond-valence sums of ⩾1.50 vu (valence units), and hence are O^{2-} anions. Ignoring any contribution from H atoms, anions at the O(1) to O(12) sites are [2]- or [3]-coordinated by Al and Cu^{2+} with incident bond-valence sums in the range 1.00–1.29 vu, and hence are $(OH)^-$ anions. Similarly, anions at the O(17) to O(19) sites are not coordinated by any metal cations in the structure; they have incident bond-valence sums of zero (omitting H atoms), and hence are (H_2O) groups.

Bond topology

The $[Al(OH)_6]$ octahedra form a $[\square Al_2(OH)_6]$ dioctahedral sheet in which half of the octahedron vacancies are occupied by Cu^{2+}, and the remaining half are vacant: $[\square Cu^{2+}Al_4(OH)_{12}]^{2+}$ (Fig. 1). Between these sheets are layers of (SO_4) groups and (H_2O) groups linked through a network of hydrogen bonds. The sheets and the layers stack along the **c** direction (Fig. 2) and are

TABLE 3. Site coordinates and displacement parameters for chalcoalumite.

Site	x	y	z	U_{11}	U_{22}	U_{33}	U_{23}	U_{13}	U_{12}	U_{eq}
Cu	0.74871(2)	0.50020(2)	0.49406(1)	0.00500(12)	0.00812(13)	0.01797(12)	–0.00068(6)	0.00255(8)	–0.00049(6)	0.01027(8)
Al(1)	0.00286(4)	0.32667(6)	0.50357(3)	0.0055(2)	0.0093(3)	0.0151(2)	–0.00019(15)	0.00200(18)	–0.00034(14)	0.00993(12)
Al(2)	0.49758(4)	0.67520(6)	0.50148(3)	0.0057(2)	0.0091(3)	0.0173(3)	0.00035(15)	0.00222(18)	0.00002(14)	0.01061(12)
Al(3)	0.25324(4)	0.16052(6)	0.49944(3)	0.0069(2)	0.0078(2)	0.0165(2)	–0.00001(15)	0.00250(18)	–0.00023(15)	0.01033(12)
Al(4)	0.24511(4)	–0.15945(6)	0.49702(3)	0.0072(2)	0.0079(2)	0.0187(3)	–0.00041(15)	0.00353(18)	–0.00053(15)	0.01109(12)
S	0.48868(4)	0.10515(5)	0.74290(2)	0.01837(19)	0.0210(2)	0.01360(18)	0.00011(14)	0.00114(14)	–0.00112(15)	0.01769(11)
O(1)	0.58554(13)	0.50007(11)	0.55216(8)	0.0089(5)	0.0102(6)	0.0154(6)	0.0002(4)	–0.0000(4)	–0.0005(4)	0.0116(2)
O(2)	0.91756(13)	0.49687(11)	0.44494(7)	0.0081(5)	0.0104(6)	0.0121(5)	–0.0005(4)	0.0008(4)	–0.0006(4)	0.0102(2)
O(3)	0.65339(12)	0.32353(13)	0.44067(7)	0.0099(5)	0.0131(6)	0.0163(5)	0.0020(4)	0.0044(4)	0.0012(4)	0.0129(2)
O(4)	0.85631(12)	0.31444(14)	0.56145(7)	0.0106(5)	0.0135(6)	0.0177(5)	–0.0043(4)	0.0063(4)	–0.0045(4)	0.0136(2)
O(5)	0.11276(12)	0.19553(14)	0.56067(7)	0.0095(5)	0.0128(5)	0.0164(5)	0.0042(4)	0.0042(4)	0.0017(4)	0.0127(2)
O(6)	0.18188(13)	0.00447(12)	0.43737(8)	0.0107(6)	0.0099(6)	0.0195(6)	–0.0005(4)	–0.0028(4)	–0.0006(4)	0.0136(3)
O(7)	0.64111(12)	0.68906(13)	0.44022(7)	0.0089(5)	0.0112(5)	0.0148(5)	–0.0019(4)	0.0032(4)	–0.0025(4)	0.0115(2)
O(8)	0.84633(12)	0.67318(13)	0.55416(7)	0.0086(5)	0.0129(6)	0.0139(5)	0.0020(4)	0.0032(4)	0.0015(4)	0.0116(2)
O(9)	–0.10271(12)	0.19348(14)	0.44411(7)	0.0091(5)	0.0121(5)	0.0176(5)	–0.0043(4)	0.0043(4)	–0.0021(4)	0.0127(2)
O(10)	0.60574(12)	0.80479(14)	0.56145(7)	0.0094(5)	0.0125(5)	0.0181(5)	–0.0046(4)	0.0045(4)	–0.0018(4)	0.0131(2)
O(11)	0.38867(11)	–0.19697(14)	0.44224(7)	0.0084(5)	0.0127(5)	0.0193(5)	0.0045(4)	0.0049(4)	0.0023(4)	0.0132(2)
O(12)	0.31366(13)	–0.00303(12)	0.55849(8)	0.0102(6)	0.0094(5)	0.0202(6)	0.0004(4)	–0.0030(4)	–0.0002(4)	0.0135(3)
O(13)	0.52462(15)	0.02155(16)	0.67381(8)	0.0269(7)	0.0240(7)	0.0184(6)	–0.0015(5)	0.0054(5)	0.0016(5)	0.0229(3)
O(14)	0.91716(19)	0.49570(17)	0.29136(9)	0.0456(10)	0.0411(9)	0.0189(7)	0.0003(6)	0.0099(7)	0.0175(7)	0.0347(4)
O(15)	0.60893(15)	0.16165(19)	0.78789(9)	0.0262(7)	0.0413(9)	0.0253(7)	–0.0018(6)	–0.0066(6)	–0.0078(6)	0.0315(3)
O(16)	0.40475(15)	0.23331(18)	0.71722(9)	0.0319(8)	0.0322(8)	0.0280(7)	–0.0015(6)	0.0004(6)	0.0124(6)	0.0309(3)
O(17)	–0.15408(15)	–0.22030(19)	0.21994(9)	0.0278(8)	0.0317(8)	0.0353(8)	0.0020(6)	0.0077(6)	0.0021(6)	0.0313(3)
O(18)	0.7238(5)	0.4046(4)	0.6941(18)	0.053(2)	0.058(2)	0.0321(14)	–0.0071(12)	0.0092(13)	–0.0225(16)	0.0473(14)
O(18A)	0.8427(7)	0.2656(9)	0.7217(4)	0.071(5)	0.090(6)	0.044(4)	–0.003(3)	0.003(3)	–0.033(4)	0.069(3)
O(18B)	0.6612(11)	0.506(2)	0.7044(4)	0.073(6)	0.27(2)	0.036(3)	–0.015(5)	0.014(3)	–0.065(9)	0.126(8)
O(19)	–0.0313(2)	0.01001(18)	0.31308(10)	0.0444(10)	0.0315(9)	0.0262(8)	0.0020(6)	–0.0013(7)	–0.0024(7)	0.0344(4)

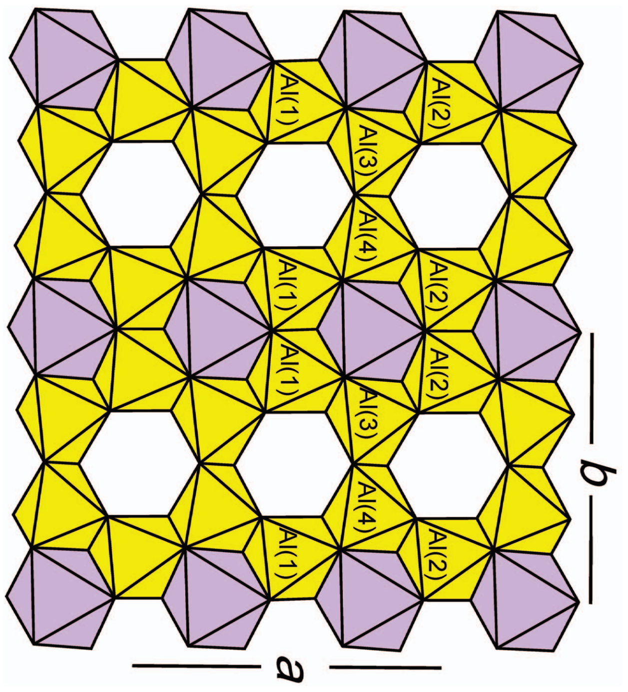

FIG. 1. The $[\square Cu^{2+}Al_4(OH)_{12}]^{2+}$ sheet in chalcoalumite; Cu polyhedra are mauve, Al polyhedra are yellow.

Table 3. (*contd.*)

Site	*x*	*y*	*z*	U_{eq}
H(1)	–0.2444(14)	–0.221(5)	0.234(2)	0.101(15)
H(2)	–0.124(4)	–0.3226(17)	0.232(2)	0.093(14)
H(5)	–0.046(3)	0.0993(18)	0.2800(14)	0.045(8)
H(6)	–0.063(4)	–0.075(3)	0.2805(19)	0.079(12)
H(7)	0.611(3)	0.495(3)	0.6089(4)	0.045(10)
H(8)	0.913(3)	0.491(3)	0.38751(16)	0.029(8)
H(9)	0.652(3)	0.313(3)	0.3836(2)	0.033(8)
H(10)	0.855(3)	0.320(3)	0.619(2)	0.044(9)
H(11)	0.097(4)	0.121(3)	0.6007(15)	0.063(11)
H(12)	0.122(3)	0.010(3)	0.3890(11)	0.045(10)
H(13)	0.624(2)	0.702(3)	0.3832(2)	0.026(7)
H(14)	0.862(3)	0.668(3)	0.61160(15)	0.032(7)
H(15)	–0.085(3)	0.128(3)	0.4003(13)	0.056(10)
H(16)	0.590(3)	0.869(3)	0.6060(12)	0.051(9)
H(17)	0.406(3)	–0.135(3)	0.3972(13)	0.056(10)
H(18)	0.382(3)	–0.005(3)	0.6029(15)	0.059(12)

TABLE 4. Selected interatomic distances (Å) in chalcoalumite.

Cu–O(1)	2.027(1)	*Al*(2)–O(1)	1.962(1)
Cu–O(2)	1.996(1)	*Al*(2)–O(1)b	1.964(1)
Cu–O(3)	2.023(1)	*Al*(2)–O(3)b	1.916(1)
Cu–O(4)	2.244(2)	*Al*(2)–O(7)	1.892(1)
Cu–O(7)	2.167(1)	*Al*(2)–O(10)	1.840(1)
Cu–O(8)	2.057(1)	*Al*(2)–O(11)c	1.828(1)
<*Cu*–O>	2.086	<*Al*(2)–O>	1.900
Al(1)–O(2)a	1.975(1)	*Al*(3)–O(5)	1.888(1)
Al(1)–O(2)b	1.943(1)	*Al*(3)–O(6)	1.856(1)
Al(1)–O(4)a	1.881(1)	*Al*(3)–O(7)b	1.952(1)
Al(1)–O(5)	1.835(1)	*Al*(3)–O(8)b	1.973(1)
Al(1)–O(8)b	1.913(1)	*Al*(3)–O(10)b	1.888(1)
Al(1)–O(9)	1.842(1)	*Al*(3)–O(12)	1.846(1)
<*Al*(1)–O>	1.898	<*Al*(3)–O>	1.901
Al(4)–O(3)d	2.034(2)	*S*–O(13)	1.475(2)
Al(4)–O(4)d	1.945(1)	*S*–O(14)f	1.468(2)
Al(4)–O(6)	1.862(1)	*S*–O(15)	1.472(2)
Al(4)–O(9)e	1.877(1)	*S*–O(16)	1.471(2)
Al(4)–O(11)	1.850(1)	<*S*–O>	1.472
Al(4)–O(12)	1.843(1)		
<*Al*(4)–O>	1.902		

a: *x*−1, *y*, *z*; b: −*x*+1, −*y*+1, −*z*+1; c: *x*, *y*+1, *z*; d: −*x*+1, −*y*, −*z*+1; e: −*x*, −*y*, −*z*+1; f: *x*−½, −*y*+½, *z*+½.

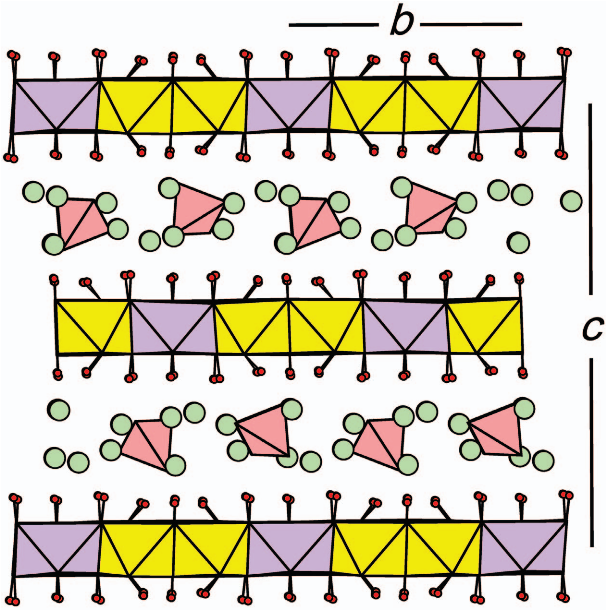

FIG. 2. Stacking of the cationic structural unit, $[\square\mathrm{Cu}^{2+}\mathrm{Al}_4(\mathrm{OH})_{12}]^{2+}$, and the anionic interstitial complex, $\{(\mathrm{SO}_4)(\mathrm{H}_2\mathrm{O})^3\}^{2-}$, along the **c** direction in chalcoalumite; Cu octahedra are mauve, Al octahedra are yellow, S tetrahedra are pink, H atoms associated with (OH) groups are shown as small red circles, $(\mathrm{H}_2\mathrm{O})$ groups are shown as large pale-green circles.

TABLE 5. Bond-valence* table for chalcoalumite.

	Cu	*Al*(1)	*Al*(2)	*Al*(3)	*Al*(4)	*S*	Σ	Anion	H(1)	H(2)	H(3) **	H(4) **	H(5)	H(6)	H(7)	H(8)	H(9)	H(10)	H(11)	H(12)	H(13)	H(14)	H(15)	H(16)	H(17)	H(18)	Σ
O(1)	0.39		0.43 0.43				1.25	(OH)							0.8												2.05
O(2)	0.42	0.42 0.45					1.29	(OH)								0.8											2.09
O(3)	0.39		0.49		0.36		1.24	(OH)									0.8										2.04
O(4)	0.22	0.54			0.45		1.21	(OH)										0.9									2.11
O(5)		0.61		0.53			1.14	(OH)											0.9								2.04
O(6)				0.57	0.43		1.00	(OH)												0.8							1.80
O(7)	0.27		0.52	0.44			1.23	(OH)													0.8						2.03
O(8)	0.36	0.49		0.42			1.27	(OH)														0.8					2.07
O(9)		0.60			0.54		1.14	(OH)															0.9				2.04
O(10)			0.60	0.53			1.13	(OH)																0.9			2.03
O(11)			0.62		0.58		1.20	(OH)																	0.8		2.00
O(12)				0.59	0.60		1.19	(OH)																		0.8	1.99
O(13)						1.50	1.50	O																0.1	0.2	0.2	2.00
O(14)						1.52	1.52	O		0.2						0.2											1.92
O(15)						1.51	1.51	O			0.1	0.1										0.2					1.91
O(16)						1.51	1.51	O	0.2				0.2								0.2						2.11
O(17)							0	(H_2O)	0.8	0.8				0.2			0.2										2.00
O(18)							0	(H_2O)			0.9	0.9			0.2			0.1									2.10
O(19)							0	(H_2O)					0.8	0.8					0.1	0.2			0.1				2.00
Σ	2.05	3.11	3.09	3.08	2.96	6.04			1.0	1.0	1.0	1.0	1.0	1.0	1.0	1.0	1.0	1.0	1.0	1.0	1.0	1.0	1.0	1.0	1.0	1.0	

* bond-valence parameters from Brown and Altermatt (1985); bond valences in vu.

** H(3) and H(4) sites were not located and refined.

linked by an extensive network of hydrogen bonds. The structure of chalcoalumite is isostructural with those of nickelalumite (Uvarova *et al.*, 2005), alvanite (Pertlik and Dunn, 1990) and ankinovichite (Karpenko *et al.*, 2004*a*). The occurrence of a cationic structural unit, $[\square Cu^{2+}Al_4(OH)_{12}]^{2+}$, and an anionic interstitial complex, $\{(SO_4)(H_2O)_3\}^{2-}$, is unusual but not unknown: similar structural motifs occur in the layered double hydroxides of the hydrotalcite super-group (Mills *et al.*, 2012), e.g. $[(AlMn^{2+}_2(OH)_6)_3]^{3+}$ and $\{(Na(H_2O)_6)(H_2O)_6(SO_4)_2\}^{3-}$ in shigaite (Cooper and Hawthorne, 1996), $[Mg_4Al_2(OH)_{12}]^{2+}$ and $\{(CO_3)(H_2O)_3\}^{2-}$ in quintinite-2H-3c (Krivovichev *et al.*, 2010).

Hydrogen bonds

The hydrogen bonding in this structure type is discussed in detail by Uvarova *et al.* (2005) who identified two types of hydrogen bonds: (1) hydrogen bonds involving the (H_2O) groups and O atoms of the (SO_4) groups; these bonds occur within the $\{(H_2O)-(SO_4)\}$ layer; (2) hydrogen bonds involving the (OH) groups of the [Cu−Al−OH] sheet and O atoms of the $\{(H_2O)-(SO_4)\}$ layer. The stereochemical details of these hydrogen bonds are given in Table 6. All H atoms are involved in strong hydrogen bonds, with H···A (acceptor) = 1.65−2.10 Å. Almost all D−H···A angles are close to 161º, typical of fairly unstrained hydrogen bonds. The O(18) (H_2O) group is partly occupied [0.697(14)] and we did not find the associated H atoms in the difference-Fourier map. The O(18) site is associated with two other partly occupied sites: O(18A) and O(18B) with occupancies of 0.350(7) and 0.436(15), respectively, and O(18)−O(18A), O(18)−O(18B) and O(18A)−O(18B) distances of 1.767(10), 1.13(2) and 2.65(2) Å. Thus O(18) and O(18A) cannot both be locally occupied, in accord with the fact that the sum of their occupancies at 1.047(16) is close to unity. Similarly, both O(18) and O(18B) cannot be locally occupied, but O(18A) and O(18B) can be locally occupied. Thus either O(18) is occupied or both O(18A) and O(18B) are locally occupied, indicating that the H_2O content of this particular crystal is somewhat in excess of 3: ~3.3 H_2O p.f.u.

TABLE 6. Hydrogen bonding in the crystal structure of nickelalumite.

D−H···A	D−A (Å)	D−H (Å)	H···A (Å)	∠D−H···A (º)
O(1)−H(7)···O(18)	2.816(4)	0.980(1)	1.94(2)	147(3)
O(1)−H(7)···O(18B)	2.640(7)	0.980(1)	1.664(8)	174(3)
O(2)−H(8)···O(14)	2.626(2)	0.980(1)	1.649(4)	174(3)
O(3)−H(9)···O(17)g	2.775(2)	0.980(1)	1.797(3)	176(2)
O(4)−H(10)···O(18)	2.873(5)	0.980(1)	2.10(2)	135(2)
O(4)−H(10)···O(18A)	2.791(6)	0.980(1)	1.84(1)	162(3)
O(5)−H(11)···O(19)e	3.014(2)	0.980(1)	2.048(8)	168(3)
O(6)−H(12)···O(19)	2.887(2)	0.980(1)	1.93(1)	164(3)
O(7)−H(13)···O(16)h	2.773(2)	0.980(1)	1.808(6)	168(2)
O(8)−H(14)···O(15)i	2.695(2)	0.980(1)	1.715(2)	179(3)
O(9)−H(15)···O(19)	2.927(2)	0.980(1)	1.952(5)	173(3)
O(10)−H(16)···O(13)c	2.906(2)	0.980(1)	1.951(9)	164(3)
O(11)−H(17)···O(13)d	2.745(2)	0.980(1)	1.782(8)	167(3)
O(12)−H(18)···O(13)	2.781(2)	0.980(1)	1.814(7)	168(3)
O(17)−H(1)···O(16)e	2.881(2)	0.980(1)	1.914(9)	169(4)
O(17)−H(2)···O(14)j	2.876(2)	0.980(1)	1.94(1)	160(4)
O(19)−H(5)···O(16)k	2.855(2)	0.980(1)	1.880(4)	173(3)
O(19)−H(6)···O(17)	2.818(3)	0.980(1)	1.850(8)	169(3)
H(1)−O(17)−H(2)	103(3)			
H(5)−O(19)−H(6)	107(3)			

a−h: see Table 4; g: $-x+\frac{1}{2}, y+\frac{1}{2}, -z+\frac{1}{2}$; h: $-x+1, -y+1, -z+1$; i: $-x+\frac{3}{2}, y+\frac{1}{2}, -z+\frac{3}{2}$; j: $x-1, y-1, z$; k: $x-\frac{1}{2}, -y+\frac{1}{2}, z-\frac{1}{2}$.

Stereochemical aspects of $^{[6]}Cu^{2+}$

Chalcoalumite

The <*Cu*–O> distance of 2.086 Å (Table 4) is short relative to that found in most other $^{[6]}Cu^{2+}$-oxysalt minerals (Burns and Hawthorne, 1996). However, Eby and Hawthorne (1993) and Burns and Hawthorne (1996) showed that <$^{[6]}$Cu–O> distances in minerals vary linearly with the degree of bond-length distortion of the octahedron away from the holosymmetric arrangement with an equal mean bond length. This type of relation is the result of the exponential form of the bond-valence interaction (Brown, 2002), and is particularly prominent for octahedrally coordinated Cu^{2+} because the degenerate electronic ground-state of a d^9 metal in a field with holosymmetric octahedral symmetry results in a spontaneous symmetry breaking and resulting distortion of the bonds away from their holosymmetric values: the Jahn-Teller effect (Jahn and Teller, 1937). Figure 3 shows the variation in <$^{[6]}$Cu–O> distance as a function of the mean-square deviation from the mean bond length for copper-oxysalt minerals. The least-squares line intercepts the ordinate at 2.083 Å (for zero distortion). This value is close to the <*Cu*–O> distance of 2.086 Å in chalcoalumite (Table 4), and accords with the low value of distortion for the associated octahedron: $\Delta = \Sigma[(l - l_o)/l_o]^2/6 = 0.002$, where l is the individual bond length and l_o is the mean bond length.

Burns and Hawthorne (1996) showed that Cu^{2+} octahedra with a very small amount of distortion away from holosymmetry commonly show strong positional disorder of their constituent anions, associated with orientational disorder of the direction of elongation of the Cu octahedra. However, this is not the case in chalcoalumite; the anions coordinating Cu^{2+} show small, relatively isotropic displacement-factors (Table 3). This indicates that the arrangement derived from the refinement is well ordered, and that we must look elsewhere for the origin of the small Jahn–Teller distortion. In this regard, it is of interest to compare the (Ni^{2+}, Zn) and Cu^{2+} octahedra in nickelalumite and chalcoalumite where the key difference between the two structures is the presence of the Jahn-Teller $^{[6]}Cu^{2+}$ in the latter. Each transition-metal octahedron is surrounded by Al octahedra with which it shares edges. Each anion in a dioctahedral [$\square Al_2(OH)_6$] sheet bonds to two Al cations and one H atom; in terms of Pauling bond strengths, it receives $0.5 \times 2 + 1.0 = 2$ vu, and there seems to be no possibility to insert a cation into a hole in the sheet. However, the bond valence at the anions may be reduced in two ways, allowing alternate occupancy of these holes by divalent transition-metals: (1) the (OH) groups are generally hydrogen-bonded to other anions in the structure and let us assume an O(donor)-H bond-valence of ~0.90 vu; (2) if only half the interstices of the [$\square Al_2(OH)_6$] sheet are occupied by a divalent metal, M^{2+} (as is the case in these structures), *Al*–O distances to anions not bonded to M^{2+} will shorten (incident bond-valence ≈ 0.90 (from H) + 2×0.55 (from Al) ≈ 2 vu). On the other hand, *Al*–O distances to anions bonded to M^{2+} will lengthen accordingly to maintain the valence-sum rule at the central *Al* site: $2 \times 0.55 + 4 \times 0.475 = 2$ vu for Al(1,2) and $4 \times 0.55 + 2 \times 0.40 = 2$ vu for Al(3,4). The resulting bond-valence incident at each of the anions bonded to M^{2+} (omitting any contribution from M^{2+} itself) is 0.90 (from H) + 2×0.40 (from Al) ≈ 1.70 vu, thus satisfying the valence-sum rule at the central M^{2+} cation with bonds of approximately the same length (Table 7, Fig. 4). However, for $^{[6]}Cu^{2+}$, there is a strong drive for [4+2]-distortion of the octahedron. In the bond topology shown in Fig. 4, there is not much compliance with regard to

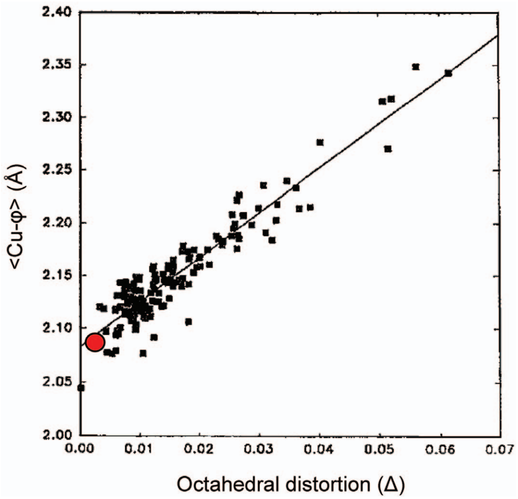

FIG. 3. <$^{[6]}Cu^{2+}$–O> distance as a function of the deviation, Δ, of the Cu–O bond lengths from their mean value, where $\Delta = \Sigma[(l - l_o)/l_o]^2/6$, l is the individual bond length and l_o is the mean bond length; the data for chalcoalumite is shown as a red circle. Modified from Burns and Hawthorne (1996).

TABLE 7. *M*-site bond lengths (Å) in nickelalumite (M = Ni, Zn) and chalcoalumite (M = Cu).

	(M = Ni,Zn)	(M = Cu)	Δ
M−O(1)	2.093	2.027	−0.066
M−O(2)	2.045	1.996	−0.049
M−O(3)	2.065	2.023	−0.042
M−O(4)	2.104	2.244	+0.140
M−O(7)	2.062	2.167	+0.105
M−O(8)	2.107	2.057	−0.050
<*M*−O>	2.079	2.086	+0.007

elongation of the central octahedron; hence there is not much possibility for changing the relative bond-valences incident to the central octahedron, and extreme distortion of the octahedron is not possible. As shown in Fig. 4*b* and Table 7 for the *Cu* site in chalcoalumite, the bonds to O(4) and O(7) are longer (weaker) with an average bond-valence of 0.25 vu whereas the equatorial bonds to O(1), O(2), O(3) and O(8) are shorter (stronger) with an average bond-valence of 0.39 vu.

Structural controls on the degree of Jahn-Teller distortion

So how do some structures containing $^{[6]}Cu^{2+}$ manage to have extremely strong Jahn-Teller distortion? The intrinsic drive to distort in this way is presumably the same in all structures as the electronic structure of Cu^{2+} is the same and the local coordination is approximately the same. The answer must lie in the structure itself. If such a distortion (elongation of an octahedron) is to be accommodated in a structure, there must be a cooperative effect whereby the linkage of the atoms can be maintained at large polyhedron distortions. There are two obvious mechanisms: (1) continuous deformation, where the Cu^{2+} octahedra can continuously deform (elongate) within the constraints of the valence-sum rule; and (2) cooperative orientational order, where the linkage of polyhedra allows large differences in bond valence within polyhedra to accord with the valence-sum rule at all the coordinating anions.

As an example of the first mechanism, consider the system $K(Mg_{1-x}Cu^{2+}_x)F_3$ which has the perovskite arrangement (Burns *et al.*, 1996). Synthetic $KMgF_3$ is cubic (space group *Pm*3*m*) whereas $KCu^{2+}F_3$ is tetragonal (space group *I*4/*mcm*). In $KMgF_3$, all Mg−F bonds are equal (1.993 Å), whereas in $KCu^{2+}F_3$, the Cu^{2+}−F bonds range from 1.85 to 2.30 Å. In solid solutions between these endmembers, the structure remains cubic in the range 1 < Mg < 0.4. In simple (Mg,Cu^{2+}) solid solutions with Cu^{2+} as a minor constituent, ESR spectroscopy has shown (e.g. Rubins and Drumheller, 1987; Rubins *et al.*, 1984) that there are local distortions around each Cu^{2+} with orientational disorder of the direction of elongation, maintaining long-range cubic symmetry (in the present case). At high concentrations of Cu^{2+} (Mg = 0.4), the strain fields

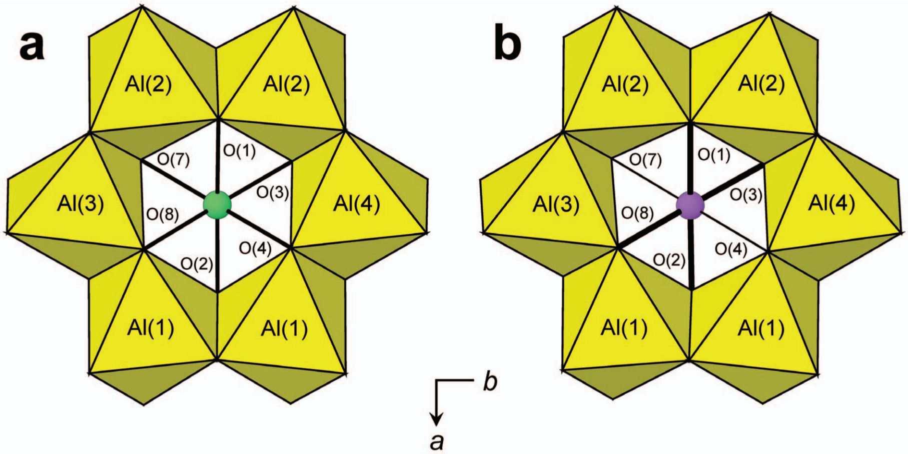

FIG. 4. Comparison of the atomic arrangements around the *Ni* and *Cu* sites in (*a*) nickelalumite, and (*b*) chalcoalumite; legend as in Fig. 2, the thickness of the Ni−O and Cu−O bonds are proportional to their bond valence.

associated with each local deformation around each Cu^{2+} couple to a vibrational phonon, there is an improper ferroelastic phase-transition, and a cooperative Jahn-Teller distortion becomes apparent in the long-range (tetragonal) structure. In $KCu^{2+}F_3$, each anion is linked to Cu^{2+} by both long (2.30 Å) and short (1.85 Å) bonds and accords with the valence-sum rule.

As examples of the second mechanism, consider the (~25) structures based on decorated $[Cu^{2+}\varphi_2]_N$ sheets (φ is an unspecified anion) (Hawthorne and Schindler, 2000). The structural unit in each of these structures consists of a close-packed sheet of octahedra of general stoichiometry $[Cu^{2+}\varphi_2]_N$ where $\varphi = (OH)^-$, Cl^-, $(H_2O)^o$, $(NO_3)^-$, $(SO_4)^{2-}$. The coordinating anions require incident bond-valence from 0 to 2 vu, and it is the presence of Jahn-Teller distortion in the Cu^{2+} octahedra that allows the wide range of structural diversity in these minerals and synthetic compounds. A key aspect of these structures is the arrangement shown in Fig. 5. In order for $(SO_4)^{2-}$ or $(H_2O)^o$ to link to three Cu^{2+} cations, the sum of the incident bond-valence at the anion must be (approximately) $\leqslant$0.5 vu. Thus the three $Cu^{2+}-\varphi$ bonds must be $\leqslant$0.17 vu, which translates to $Cu^{2+}-\varphi \geqslant 2.34$ Å. Minor variations in the lengths of the S−O bonds and variation in the strength of hydrogen bonding involving the (H_2O) groups allows large variation in the lengths of the $Cu^{2+}-\varphi$ bonds. For example, a strong S−O bond (1.7 vu) will result in an average $Cu^{2+}-\varphi$(apical) bond length of 2.53 Å, and an (H_2O) group with weak hydrogen-bonds (0.05 vu) will result in an average $Cu^{2+}-\varphi$(apical) bond length of 2.94 Å. The remaining anions, $(OH)^-$, Cl^-, in the $[Cu^{2+}\varphi_2]_N$ sheet require $\geqslant$1 vu from the Cu^{2+} cations, and are equatorial anions of the Cu^{2+} octahedra. It is the cooperative orientational order of the locally associated Jahn-Teller distortions that allows large axial distortions of octahedra within a continuous structure.

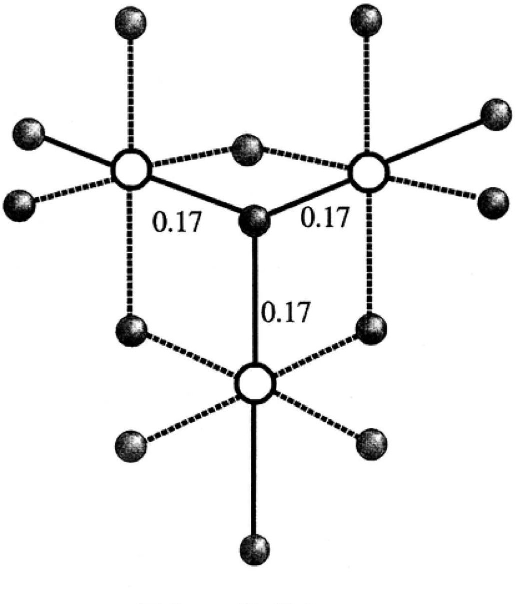

FIG. 5. Typical local bond-valence arrangement for an $(SO_4)^{2-}$ or $(H_2O)^o$ group to link to a $[Cu^{2+}\varphi_2]_N$ sheet; Cu^{2+} cations are shown as white circles, anions are shown as highlighted dark circles, bond valences are shown around the central anion, apical (elongated) bonds are shown as full lines, equatorial bonds are shown as dotted lines. Note that three apical (long) $Cu^{2+}-\varphi$ bonds must link to the same anion to provide an incident bond valence, A, appropriate for $\varphi = (SO_4)^{2-}$ or $(H_2O)^o$. From Hawthorne and Schindler (2000).

Acknowledgements

This work was supported by a Canada Research Chair in Crystallography and Mineralogy, Research Tools and Equipment, and Discovery Grants from the Natural Sciences and Engineering Research Council of Canada, and Canada Foundation for Innovation Grants, both to FCH.

References

Agakhanov, A.A., Karpenko, V.Y., Pautov, L.A., Uvarova, Y.A., Sokolova, E., Hawthorne, F.C. and Bekenova, G.K. (2005) Kyrgyzstanite, $ZnAl_4(SO_4)(OH)_{12}(H_2O)_3$ – a new mineral from the Kara-Tangi, Kyrgyzstan. *New Data on Minerals*, **40**, 23−28.

Brown, I.D. (2002) *The Chemical Bond in Inorganic Chemistry. The Bond Valence Model*. International Union of Crystallography Monographs on Crystallography, **12**. Oxford University Press, USA.

Brown, I.D. and Altermatt, D. (1985) Bond-valence parameters obtained from a systematic analysis of the inorganic crystal structure database. *Acta Crystallographica*, **B41**, 244−247.

Bruker Analytical X-ray Systems (1997) *SHELXTL Reference Manual 5.1.*, Bruker AXS Inc., Madison, Wisconsin, USA.

Burns, P.C. and Hawthorne, F.C. (1996) Static and dynamic Jahn-Teller effects in Cu^{2+}-oxysalt minerals. *The Canadian Mineralogist*, **34**, 1089−1105.

Burns, P.C., Hawthorne, F.C. and Hofmeister, A.M.

(1996) A structural phase transition in $K(Mg_{1-x}Cu_x)F_3$ perovskite. *Physics and Chemistry of Minerals*, **23**, 141−150.

Cooper, M.A. and Hawthorne, F.C. (1996) The crystal structure of shigaite, $[AlMn^{+}(OH)_6]_3(SO_4)_2Na(H_2O)_6\{H_2O\}_6$, a hydrotalcite-group mineral. *The Canadian Mineralogist*, **34**, 91−97.

Eby, R.K. and Hawthorne, F.C. (1993) Structural relations in copper oxysalt minerals. I. Structural hierarchy. *Acta Crystallographica*, **B49**, 28−56.

Frost, R.L., Reddy, B.J. and Keeffe, E.C. (2010) Structure of selected basic copper(II) sulphate minerals based on spectroscopy. Implications for hydrogen bonding. *Journal of Molecular Structure*, **977**, 90−99.

Hawthorne, F.C. and Schindler, M. (2000) Topological enumeration of decorated $[Cu^{2+}\varphi_2]_N$ sheets in hydroxy-hydrated copper-oxysalt minerals. *The Canadian Mineralogist*, **38**, 751−761.

Hawthorne, F.C., Krivovichev, S.V. and Burns, P.C. (2000) The crystal chemistry of sulfate minerals. Pp. 1−112 in: *Sulfate Minerals: Crystallography, Geochemistry, and Environmental Significance* (C.N. Alpers, J.L. Jambor and D.K. Nordstrom, editors). Reviews in Mineralogy and Geochemistry, **40**, Mineralogical Society of America and Geochemical Society, Washington, D.C.

Jahn, H.A. and Teller, E. (1937) Stability of polyatomic molecules in degenerate electronic states. I. Orbital degeneracy. *Proceedings of the Royal Society of London. Series A, Mathematical and Physical Sciences*, **161(905)**, 220−235.

Karpenko, V.V., Pautov L.A., Sokolova, E., Hawthorne, F.C., Agakhanov, A.A., Dikaya, T.V. and Bekenova, G.K. (2004*a*) Ankinovichite, nickel analogue of alvanite, a new mineral from Kurunsak (Kazakhstan) and Kara-Chagyr (Kirgizia). *Zapiski Vsesoyuznogo Mineralogicheskogo Obshchestva*, **133**, **N2**, 59−70.

Karpenko, V.V., Agakhanov, A.A., Pautov, L.A., Dikaya, T.V. and Bekenova, G.K. (2004*b*) New occurrence of nickelalumite on Kara-Chagyr, South Kirgizia. *New Data on Minerals*, **39**, 32−39.

Krivovichev, S.V., Yakovenchuk, V.N., Zhitova, E.S., Zolotarov, A.A., Pakhomosky, Y.A. and Ivanyuk, G.Yu. (2010) Crystal chemistry of natural layered double hydroxides. 1. Quintinite-2H-3c from the Kovdor alkaline massif, Kola peninsula, Russia. *Mineralogical Magazine*, **74**, 821−832.

Larsen, E.S. and Vassar, H.E. (1925) Chalcoalumite, a new mineral from Bisbee, Arizona. *American Mineralogist*, **10**, 79−83.

Martini, J.E.J. (1980) Mbobomkulite, hydrombobomkulite, and nickelalumite, new minerals from Mbobo Mkulu cave, eastern Transvaal. *Annals of the Geological Survey of South Africa*, **14**, 1−10.

Mills, S.J., Christy, A.G., Genin, J.-M.R, Kameda, T. and Colombo, F. (2012) Nomenclature of the hydrotalcite supergroup: natural layered double hydroxides. *Mineralogical Magazine*, **76**, 1289−1336.

Pertlik, F. and Dunn, P.J. (1990) Crystal structure of alvanite, $(Zn,Ni)Al_4(VO_3)_2(OH)_{12}\cdot 2H_2O$, the first example of an unbranched zweier-single chain vanadate in nature. *Neues Jahrbuch für Mineralogie, Monatshefte*, **9**, 385−392.

Rubins, R.S. and Drumheller, J.E. (1987) The temperature dependence of the EPR spectrum of Cu^{2+} in $ZnTiF_6.6H_2O$ between 4 and 160 K. *Journal of Chemical Physics*, **86**, 6660−6664.

Rubins, R.S., Tello, L.N., De, D.K. and Black, T.D. (1984) Jahn-Teller EPR spectra of Cu^{2+} in $MgSiF_6.6H_2O$ between 4 and 160 K. *Journal of Chemical Physics*, **81**, 4230−4233.

Sheldrick, G.M. (2008) A short history of SHELX. *Acta Crystallographica*, **A64**, 112−122.

Uvarova, Y.A., Sokolova, E., Hawthorne, F.C., Karpenko, V., Agakhanov, A.A. and Pautov, L.A. (2005) The crystal chemistry of the “nickelalumite”-group minerals. *The Canadian Mineralogist*, **43**, 1511−1519.

Williams, S. and Khin, B.S. (1971) Chalcoalumite from Bisbee, Arizona. *Mineralogical Record*, **2**, 126−127.